Simulation of Magnetization Errors Using Conformal Mapping Field Computations

Peter Offermann[1], Martin Hafner[2], and Kay Hameyer[1]

[1]Institute of Electrical Machines, RWTH Aachen University, D-52062, Aachen, Germany
[2]Schabmüller GmbH, D-92334, Berching, Germany

Due to their production and magnetization process, rare earth magnets, e.g. NdFeB, exhibit deviations from the targeted ideal remanent magnetic flux-density. As a consequence, the calculation of cogging torque, load torque and force computations of a permanent-magnet synchronous machine by means of finite-element analysis are at best in fair agreement to measurements, since the mentioned variations of the magnet material are not covered by standard simulation models. Actual solutions to consider these variations in the simulation of a permanent-magnet synchronous machine consist either in a full-factorial Monte-Carlo simulation or advanced stochastic analysis techniques such as the creation of polynomial-chaos meta-models. Even meta-model techniques result in an exponential growth of repetitive finite element simulations for a rise in the used polynomial's degree or an increment of the input variables. In order to reduce computation time, this paper unveils a methodology to build the magnet rotor field distribution with consideration of magnet faults semianalytically for calculating arbitrary machine operation points. For this purpose a conformal mapping approach is extended to be applicable to stochastic variations. It is shown, how the conformal mapping assumption of symmetrical field conditions can be overcome. As a result, the proposed approach is applied to the calculation of cogging torques for stochastic varying magnetizations in a permanent synchronous machine.

***Index Terms*—Conformal mapping, finite element method, magnetization error simulation, stochastic field analysis.**

I. Introduction

DUE to their production and magnetization process, rare earth high energy magnets, e.g. NdFeB, exhibit a deviation from the targeted ideal remanent magnetic flux-density [1]. Fig. 1 shows such variations for the measured radial, outward-pointing flux-density from a batch of 26 arc-segment permanent-magnets with diametral magnetization. Typical solutions to consider these variations in the simulation of a PMSM consist either of worst-case estimations or of full-factorial Monte-Carlo simulations. Even in recent advances such as the application of nonintrusive polynomial-chaos meta-models [2], sample points from the original model—their number depending on the number of input random variables and the meta-model's polynomial degree—need to be calculated in order to create the desired meta-model. The meta-model itself is used to subsequently calculate the Sobol-indices to perform a sensitivity analysis.

Let us assume that the given magnetization curves from Fig. 1 can be approximated by an error model which employs two random variables [3]. For a PMSM with three pole-pairs this implies a number of $M = 12$ random variables. Assuming furthermore that a polynomial of order $n = 2$ is used for calculation, applying a tensor-product quadrature scheme, $N = (n+1)^M = 531,441$ FE-model evaluations are required for the meta-model's creation [4]. Even if more efficient evaluation-point selection algorithms are applied, complete machine calculations require the inclusion of further random variables, describing possible geometry variations or material data changes.

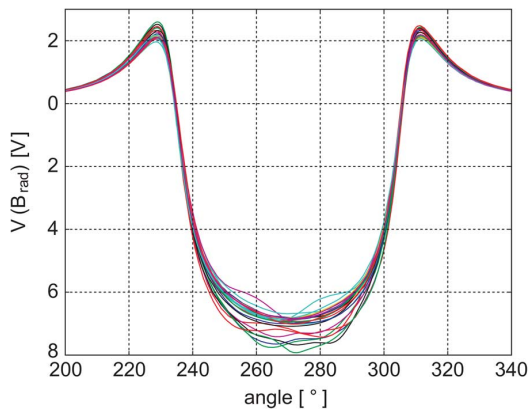

Fig. 1. Hall-voltages of measured radial, outward-pointing flux-densities from a batch of 26 arc-segment permanent-magnets with diametral magnetization, taken 1.5 mm above the magnet's surface.

Due to the exponential growth in this problem, even parallelization (at best resulting in a linear speedup) cannot solve this so-called curse of dimensionality.

Recent publications showed that the air gap field of surface-mounted PMSMs can be computed for an arbitrary operation point in case of linear material behavior by semianalytic conformal mapping approaches [5], leading to computation times below a second. These techniques are due to the assumption of linear time invariance (LTI) comparable to [6]. Excluding the armature reaction, the CM approach can be generalized to PMSM having a random buried magnet topology [7]. To utilize the advantages of these approaches in stochastic variation simulations, one has to overcome the assumption of symmetrically field conditions (e.g. the field distribution of different magnetic poles differs in function of the stochastic input parameters).

This paper unveils a methodology to build a rotor field distribution semianalytically in order to account for nonsymmetric excitation variations. It has been applied for a magnet model

Manuscript received October 30, 2012; revised January 11, 2013; accepted January 14, 2013. Date of current version July 15, 2013. Corresponding author: P. Offermann (e-mail: peter.offermann@iem.rwth-aachen.de).

Color versions of one or more of the figures in this paper are available online at http://ieeexplore.ieee.org.

Digital Object Identifier 10.1109/TMAG.2013.2242196

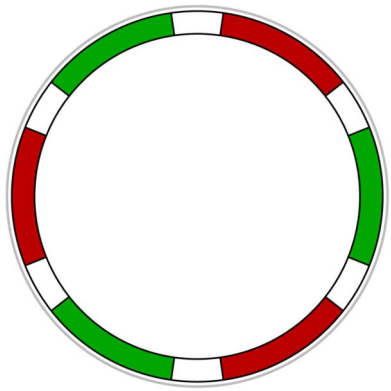

Fig. 2. Geometry of applied FEA for the simulation of ${}^{r}\underline{B}(\Theta)$. The outer gray circle represents the applied Neumann boundary-condition, acting as an infinite permeable, slottless stator.

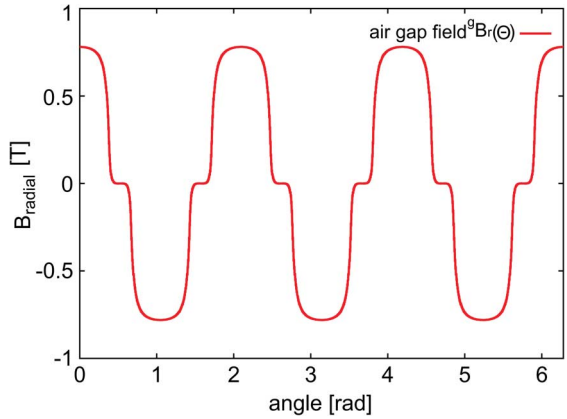

Fig. 3. Radial component of the air gap field from the rotor of Fig. 2, featuring six ideal-unidirectional magnetized magnets.

having two random variables on a PMSM featuring 3 pole-pairs and stator with 18 teeth to calculate the influence on cogging torque. This allows bringing valuable insight for sensitivity analysis by adding cause-effect correlation and reducing the number of necessary FEA simulations by a factor larger than thousand for the execution of a full-factorial parameter sweep.

II. Methodology

The calculation of all possible magnet-error permutations applying FEA is—independent of the applied method for uncertainty propagation—unfeasible, because the necessary computational effort rises exponentially (Section I) and leads to unbearable calculation times even for 2D-models. The problem of calculating all magnet-error permutations however can be split into the much smaller task of calculating all occurring variations for only one magnet and reconstructing the rotor ansatz-function for hybrid CM-computations applying the principle of superposition as discussed in the following section.

A. Conformal Mapping

The principle of conformal mapping approaches [8] consists of a separation of the air gap field ${}^{g}\underline{B}$ into its main contributing components:

- the air gap field excitation of the rotor ${}^{r}\underline{B}(\Theta)$ in dependence of the coordinate angle $\Theta \in [0, 2\pi[$ under the assumption of an unslotted, infinite permeable stator;
- the influence of the stator's slotting onto the rotor's unslotted-stator air gap field, described by the permeance-function $\underline{\lambda}$;
- the stator's air gap field field excitation ${}^{a}\underline{B}(\vec{I})$ created by the symmetric three-phase current $\vec{I}$.

All described, contributing components are complex-valued quantities with their real part[1] representing the radial, outwards-pointing and the complex part[2] representing the tangential field component. The resulting air gap field, in this paper restricted to linear material behavior, can then calculated by

$$ {}^{g}\underline{B}(\Theta, \vec{I}) = {}^{r}\underline{B}(\Theta) \cdot \underline{\lambda}^{*} + {}^{a}\underline{B}(\vec{I}) \tag{1} $$

B. Rotor Ansatz-Functions With Ideal Pole Superposition

Classic CM employs analytical, infinite-Fourier-series decompositions to generate a rotor field description [9]. Analytical calculation of the rotor field for arbitrary magnetization errors however is at best unrewarding, more likely impossible. Hence the field ${}^{r}\underline{B}(\Theta)$ is extracted from a FEA. For these simulations, the stator can be replaced by a Neumann boundary-condition. This forces the magnetic field's tangential component $H_{\varphi}(\Theta)$ to zero and ergo acts in the same way as an infinite permeable, slottless stator (Fig. 2).

Instead of simulating the three pole pairs, the system's LTI-property also enables to split the FEA into p separate simulations, where in each simulation only one magnet is simulated. The air gap field then equals the accumulation of all p separate simulations. Since all magnets in the simulation of an ideal rotor are equal, one simulation of one magnet in the given geometry suffices to create the complete superposition

$$ \underline{B}(\Theta) = \sum_{i=1}^{p} \underline{B}_i z/(\Theta) = \sum_{i=1}^{p} \left[\underline{B}_1 \left(\Theta + 360 \frac{i}{p} \right) (-1)^{(i+1)} \right]. \tag{2} $$

A comparison of an analytical air gap field calculation with an air gap field reconstructed from only one magnet's FEA simulation verifies these considerations and yields the extracted radial field component depicted in Fig. 3.

[1]denoted by the subscript index r

[2]denoted by the subscript index φ

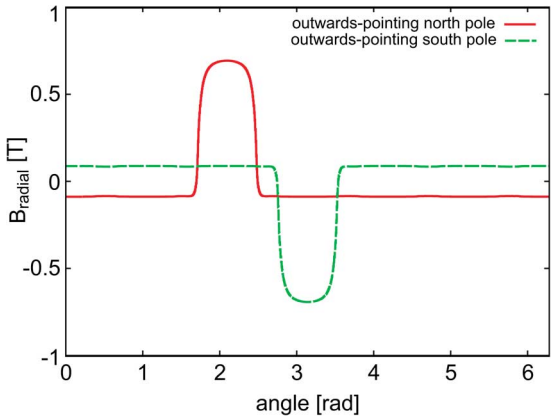

Fig. 4. Extraction of the ${}^{r}B_r(\Theta)$-field taken from two single-magnet simulations, their sum building a pole-pair.

III. Results

A. Error Pole Superposition

In order to apply the proposed pole superposition principle for erroneous magnets, the central question to be clarified is whether

$$\nabla \cdot \underline{B} = 0 \tag{3}$$

stays valid for unsymmetrical excited rotor systems. A careful analysis of the per-pole FEA simulations solves this problem:

Fig. 4 shows the radial air gap field ${}^{r}B_r(\Theta)$ of two per-pole magnet simulations. An integration over the air gap field created by one single magnet proves, that (3) stays valid, whatever changes are applied to the magnet. A subsequent application of the system's LTI-property proves, that (3) keeps validity for the superposition of unsymmetrical excitations, too. An addition of both curves finally yields the excitation of one pole pair, as can be seen in a comparison to Fig. 3.

B. Application Conditions

To keep comparability to previous works [10], the machine geometry presented in Fig. 5 has been employed. The implemented magnet variation model comprises two error possibilities [3]: Global changes of the magnet's remanence flux-density (random-variable ξ_1) and position-dependent angle errors of the magnetic flux-density (random variable ξ_2). For the sake of an impact estimation of these variations onto cogging torque, each random variable is allowed to adopt only two values—either its ideal value or its maximum deviation with the following probabilities:

$$p(\xi_1 = 0.95) = 0.33 \qquad p(\xi_1 = 1) = 0.67$$
$$p(\xi_2 = -0.2) = 0.5 \qquad p(\xi_2 = 0.0) = 0.5.$$

Fig. 6 illustrates the error cases with maximum error for both random variables, applying a global remanence flux-density weakening of 5% ($\xi_1 = 0.95$) and an angle compression of 10° ($\xi_2 = -0.2$) at the magnet's outer edge in comparison to an ideal magnetization. Whereas the global flux-density weakening only results in a scaling factor for the air gap field, the angle error generates deviations of the air gap field's shape which are best visible at the magnet's edges and its middle. Fig. 7 shows the reconstructed ${}^{r}B_r(\Theta)$-field with the first error implemented for the pole located at 2.1[rad] and the second error located at the 4.2[rad], all other poles ideal. Both errors poles do not influence the field of the other poles, however lead to a small offset of the overall air gap field.

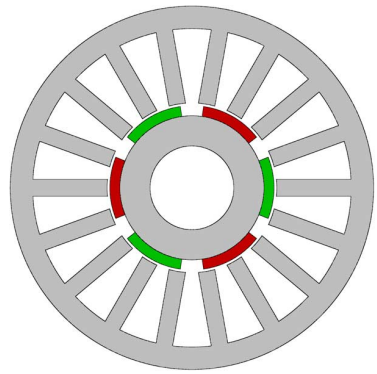

Fig. 5. Cross-section of the employed machine geometry for simulation, having 18 stator teeth and three pole pairs with unidirectional, variably defective magnetizations.

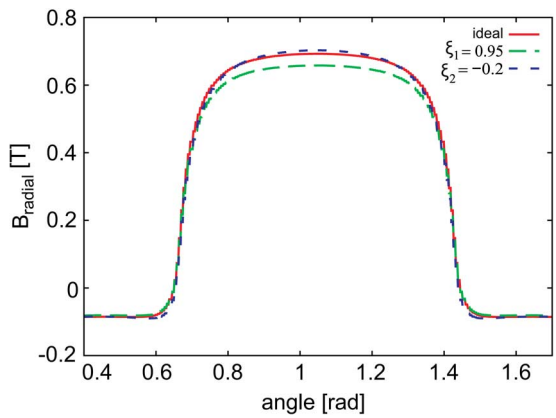

Fig. 6. Influence of the considered magnet errors onto the ${}^{r}B_r(\Theta)$-field for one magnet in comparison to an ideal magnetization.

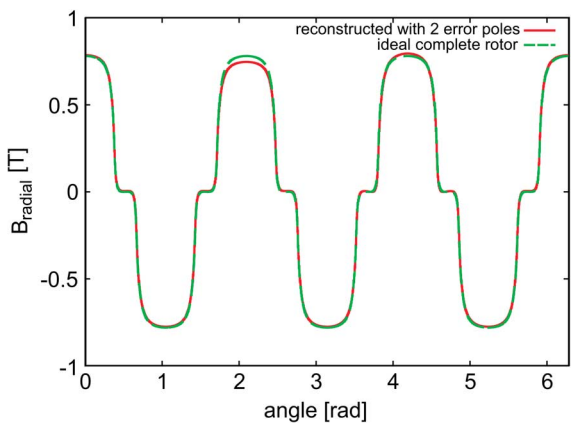

Fig. 7. Reconstructed ${}^{r}B_r(\Theta)$-field with the error poles form Fig. 6 located at 2.1[rad] and 4.2[rad], all other poles without variation.

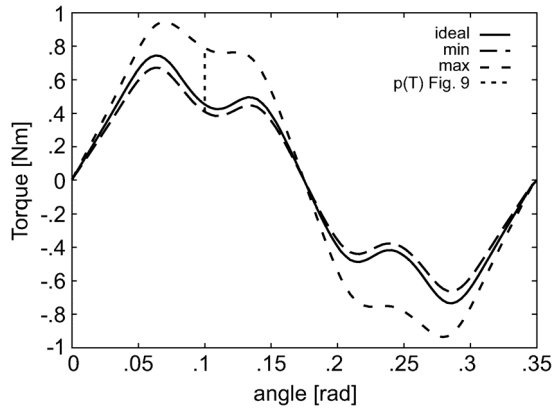

Fig. 8. Maximal and minimal cogging torque of all possible error combinations in comparison to the ideal rotor without magnet deviations.

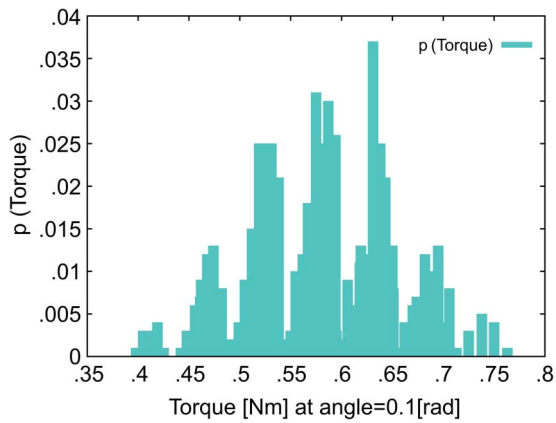

Fig. 9. Histogram of cogging torques at angle 0.1[rad].

C. Variation Analysis

For these simple conditions, a calculation of all possible rotor combinations would result in $4^6 = 4096$ possible models. Allowing a reduction by symmetry considerations[3] of a factor 32, we assume that 128 relevant constellations still would have to be considered. Because cogging torque requires high angle resolutions, we consider a spatial discretization of 100 rotor steps over one cogging torque period. As a consequence, still 12.800 FEA-simulations are necessary with the exploitation of symmetries.

Applying the proposed hybrid conformal mapping superposition approach, 4 FEA-simulations are necessary to extract all possible per-pole rotor ansatz-functions and 1 FEA-simulation to extract the permeance ansatz-function. The creation of all rotor-ansatz functions requires only a number of summations which can be neglected when compared to an FEA. The cogging torque calculation per rotor movement angle also requires no recomputation of the created rotor-ansatz functions, only array shifts which—once again—can be neglected. In total, the required number of FEA can be reduced by a factor of 2.560. Fig. 8 depicts the resulting histogram error envelope of all possible rotor variations and Fig. 9 shows the corresponding probabilities along the cut at angle 0.1.

[3]which often are tedious and error prone

IV. Conclusion

This paper proposes to apply the superposition of hybrid CM ansatz-functions, in order to decrease the computational complexity of variational calculations, which always are required for stochastic system evaluations. The validity of the model has been explained for the case of linear materials, improvements towards nonlinear material calculations are ongoing. The proposed method has been demonstrated on the example of magnetization faults. It's application reduced the number of required FEAs for a complete cogging torque analysis dramatically and enabled a cogging torque analysis for more than 4000 machine variations in a calculation time of below 2 minutes. Finally, the proposed, versatile approach is not restricted to magnet variations but could also be applied for current or material changes, where those changes are moved into the corresponding current or permeance ansatz functions.

Acknowledgment

The results presented in this paper have been developed in the research project "Propagation of uncertainties across electromagnetic models" granted by the Deutsche Forschungsgemeinschaft (DFG).

References

[1] F. Jurisch, "Production process based deviations in the orientation of anisotropic permanent magnets and their effects onto the operation performance of electrical machines and magnetic sensors," in *Proc. Int. ETG-Kontress Tagungsband, (ETG-FB 107)* (in German), 2007, no. 1, pp. 255–261.

[2] R. Ghanem and P. Spanos, *Stochastic Finite Elements: A Spectral Approach*, ser. Civil, Mechanical and Other Engineering Series. New York: Dover, 2003.

[3] P. Offermann and K. Hameyer, "Comparison of physical and non-physical magnetisation fault approaches," in *Proc. 12th Int. Workshop Optimiz. Inverse Problems Electromagnetism*, Sep. 2012, pp. 156–157.

[4] B. Sudret, "Uncertainty Propagation and Sensitivity Analysis in Mechanical Modesl—Contributions to Structural Reliability and Stochastic Spectral Methods," Ph.D. dissertation, Ecole Doctorale Sciences pour l'Ingenieur, Universite BLAISE PASCAL—Clermont II, , 2007.

[5] M. Hafner, D. Franck, and K. Hameyer, "Static electromagnetic field computation by conformal mapping in permanent magnet synchronous machines," *IEEE Trans. Magn.*, vol. 46, no. 8, pp. 3105–3108, Aug. 2010.

[6] W. Zhu, B. Fahimi, and S. Pekarek, "A field reconstruction method for optimal excitation of permanent magnet synchronous machines," *IEEE Trans. Energy Convers.*, vol. 21, no. 2, pp. 305–313, Jun. 2006.

[7] D. Franck, M. Hafner, and K. Hameyer, "Computational cost-effective modelling of non-linear characteristics in permanent magnet synchronous motors," *COMPEL*, vol. 30, no. 3, pp. 885–893, May 2011.

[8] D. Zarko, D. Ban, and T. Lipo, "Analytical solution for cogging torque in surface permanent-magnet motors using conformal mapping," *IEEE Trans. Magn.*, vol. 44, no. 1, pp. 52–65, Jan. 2008.

[9] Z. Zhu, D. Howe, E. Bolte, and B. Ackermann, "Instantaneous magnetic field distribution in brushless permanent magnet dc motors. i. open-circuit field," *IEEE Trans. Magn.*, vol. 29, no. 1, pp. 124–135, Jan. 1993.

[10] M. Hafner, D. Franck, and K. Hameyer, "Conformal mapping approach for permanent magnet synchronous machines: On the modeling of saturation," *Arch. Electr. Eng.*, vol. 61, no. 2, pp. 211–220, Jun. 2012.